THE ASTROPHYSICAL JOURNAL, 189:89–100, 1974 April 1

INFRARED FLUXES, SPECTRAL TYPES, AND TEMPERATURES FOR VERY COOL STARS

H. M. DYCK,* G. W. LOCKWOOD†
Kitt Peak National Observatory‡
AND
R. W. CAPPS
Kitt Peak National Observatory‡ and Steward Observatory, University of Arizona
Received 1973 August 23; revised 1973 October 26

ABSTRACT

From narrow- and broad-band photometry between 0.55 and 10.2 μ, complete energy distributions, photometric spectral types, and total fluxes are derived for a sample of cool giants, Mira variables, and IRC stars. From stars lacking infrared excesses, an intrinsic relation for color temperature versus spectral type is found for M0–M10 stars as well as bolometric corrections for the fluxes at 1.04 and 2.2 μ. The effective temperature scale for cool stars is reexamined and its sources of error are discussed.

Subject headings: infrared sources — late-type stars — long-period variables — photometry

I. INTRODUCTION

When the catalog of infrared sources resulting from the California Institute of Technology 2-μ sky survey (called the IRC) was published (Neugebauer and Leighton 1969), there were over 1000 sources for which no optical counterparts were listed. Grasdalen and Gaustad (1971) were able to reduce the number of unidentified objects north of declination $-4°$ to 235 by cross-correlating the IRC positions with positions of stars given in the *Dearborn Catalogue of Faint Red Stars* and in the Case infrared surveys of the galactic plane. The remaining unidentified sources were among the reddest stars in the IRC typically having apparent $I - K$ colors greater than 4 mag. Some of these stars have recently been identified with named variable stars by Kukarkin (1972) and by Lockwood and Zinter (1973). Slitless spectra for most of the unidentified sources in Grasdalen and Gaustad's list were obtained by Vogt (1973) who determined that the overwhelming majority of them were of late M spectral type. Near-infrared photometry by Lockwood and McMillan (1971) and Lockwood (1973) confirms this result and further identifies a small extraordinarily reddened set of M supergiants and carbon stars. Evidence of microwave emission (Wilson and Barrett 1971) and circumstellar shells (Ulrich *et al.* 1966; Dyck, Forbes, and Shawl 1971) has been found for some of the reddest IRC stars.

Because the reddest IRC stars appear to represent a set of objects with more extreme characteristics than those of the relatively normal Mira variables and giants of roughly the same range of spectral types, we decided to investigate the photometric properties of a sample of these stars. Crucial to the success of this endeavor, in our judgment, was the near-simultaneous measurement of as much as possible of the complete energy distributions *and* the photometric spectral types. This was accomplished by means of broad-band photometry from 0.55 to 10.2 μ to determine the energy distributions coupled with narrow-band photometry in the 0.78- to 1.05-μ region to determine the spectral types.

This paper presents results of the photometry of a sample of IRC stars, normal Miras, and cool giants, and a new discussion of the color temperatures, effective temperatures, total fluxes, and "bolometric" flux corrections for cool stars.

II. OBSERVATIONS

The data were obtained with the Kitt Peak National Observatory 0.9- and 1.3-meter telescopes during 1971 using three different photometric systems. Infrared observations at 1.25, 1.65, 2.2, and 3.4 μ were made with a lead sulfide detector, while observations at 2.2, 3.4, 5.0, and 10.2 μ employed a gallium-doped germanium bolometer. The broad-band filters used duplicated as far as possible the standard *J*, *H*, *K*, *L*, *M*, and *N* passbands. In the visible and near-infrared regions, data were obtained with an S-1 photomultiplier and various photometers using a broad-band filter combination at 0.55 μ approximating the *V* passband, and narrow-band filters at 0.78, 0.87, 0.88, 1.04, and 1.05 μ. The latter were chosen to isolate TiO and VO molecular bands and nearby relatively uncontaminated continuum regions in M stars so that photometric spectral types can be determined from the band strengths.

Wing (1967) has shown that the region around 1.04 μ is the best continuum point accessible to conventional photometry in cool M stars, so that the fluxes obtained at this wavelength are of great importance in the

* Now at Institute for Astronomy, Honolulu, Hawaii.
† Now at Lowell Observatory, Flagstaff, Arizona.
‡ Operated by the Association of Universities for Research in Astronomy, Inc., under contract with the National Science Foundation.

TABLE 1

Infrared Observations

Star	JD (2440000+)	$.55\mu$	$.78\mu$	$.87\mu$	$.88\mu$	1.04μ	1.05μ	1.25μ	1.65μ	2.2μ	3.4μ	5.0μ	10.2μ	Spectral Type	log F (W cm^{-2})
		log F_λ (W cm$^{-2}\mu^{-1}$)													
-30217	1050	-17.73	-15.83	-15.23	-15.15	-14.45	-14.75		-14.36	-14.55	-14.92		-15.98	M9.8	-14.00*
-30217	1107	-16.91	-15.29	-14.74	-14.68	-14.14	-14.36			-14.50	-14.82	-15.23	-15.79	M9.3	
-20293	1051	-16.24	-15.05	-14.46	-14.48	-14.08	-14.11		-13.96	-14.29	-14.81		-16.52	M7.9	-13.74*
-10236	1049	-16.77	-15.53	-15.40	-15.38	-15.21	-15.18		-14.48	-14.16	-14.01		-14.81	C	
+00028	1215	-15.76	-14.74	-14.15	-14.20	-13.83	-13.86	-13.74	-13.82	-14.14	-14.70	-15.31	-16.03	M7.9	-13.56
+00266	1050	-18.24	-16.47	-15.74	-15.66	-14.92	-15.18		-14.57	-14.73	-15.10		-16.24	M9.6	-14.25*
+00266	1107	-18.51	-16.66	-15.87	-15.78	-15.01	-15.31			-14.93	-15.28			M9.9	
+00281	1049	-15.94	-14.92	-14.36	-14.40	-14.04	-14.06		-13.97	-14.31	-14.91			M7.8	
+10011	1251			-17.09		-15.95	-16.23	-15.43	-14.78	-14.28	-14.02				
+10050	1277	-16.35	-14.46	-13.81	-13.72	-12.98	-13.22	-12.90	-12.86	-13.02	-13.26			M9.5	
+10313	1215	-16.69	-15.43	-14.83	-14.85	-14.34	-14.43	-14.21	-14.23	-14.53	-15.06			M8.4	
+10523	1215	-16.53	-14.99	-14.39	-14.38	-13.80	-13.99	-13.70	-13.76	-14.00	-14.40	-14.78	-15.18	M9.1	-13.40
+10523	1251	-16.68	-15.12	-14.50	-14.47	-13.82	-14.03	-13.74	-13.78	-14.03	-14.43			M9.2	
+10525	1251	-17.22	-15.40	-14.72	-14.71	-14.22	-14.32	-14.14	-14.14	-14.29	-14.54		-15.35	M8.5	
+20052	1215	-16.09	-14.85	-14.25	-14.28	-13.82	-13.87	-13.65	-13.68	-13.97	-14.49	-15.04	-15.91	M8.1	-13.42
+20281	1109	-18.24	-16.68	-15.96	-15.89	-15.15	-15.36			-14.58	-14.69		-15.58	M9.3	
+20328	1106	-17.53	-15.70	-15.06	-14.98	-14.26	-14.54			-14.24	-14.52		-15.58	M9.8	
+30021	1106	-17.81	-15.85	-15.16	-15.13	-14.49	-14.64			-14.41	-14.71	-15.09	-15.38	M8.9	
+30021	1214		-16.21	-15.57	-15.48	-14.77	-14.99	-14.50	-14.36	-14.52	-14.82	-14.97	-15.42	M9.4	-13.89
+30021	1251	-18.37	-16.38	-15.65	-15.58	-14.84	-15.09	-14.58	-14.47	-14.57	-14.86			M9.6	
+30021	1277		-16.51	-15.80	-15.70	-14.93	-15.19	-14.63	-14.49	-14.62	-14.91			M9.7	
+30055	1215	-16.40	-15.15	-14.55	-14.60	-14.17	-14.19	-14.03	-14.05	-14.34	-14.88	-15.28	-16.13	M7.9	-13.78
+30292	1074		-16.12	-15.44	-15.40	-14.74	-14.84		-14.36	-14.41	-14.63	-15.12	-15.44	M8.6	-13.87
+30292	1215		-16.72	-16.00	-15.89	-15.16	-15.41	-14.86	-14.64	-14.67	-14.90	-15.10	-15.57	M9.6	-14.06
+30515	1215	-15.61	-14.49	-13.90	-13.96	-13.57	-13.60	-13.45	-13.51	-13.83	-14.39	-14.88	-15.75	M7.9	-13.25
+40004	1215			-16.29	-16.24	-15.23	-15.36	-14.56	-14.24	-14.21	-14.34	-14.45	-14.86		-13.51
+40004	1251	-18.20	-17.27	-16.31	-16.25	-15.33	-15.49	-14.68	-14.32	-14.28	-14.41		-15.06	M9.1	
+40442	1251	-17.35	-15.57	-14.88	-14.81	-14.12	-14.34	-13.86	-13.79	-14.01	-14.46		-15.83	M9.3	
+40448	1215		-16.54	-15.71	-15.74	-15.05	-15.01	-14.56	-14.04	-13.65	-13.45	-13.50	-13.71	M7.0	-12.63
+40485	1215	-16.76	-15.41	-15.22	-15.18	-14.97	-14.94	-14.65	-14.34	-14.18	-14.26	-14.36	-15.04	C	-13.47
+40485	1251	-16.60	-15.29	-15.12	-15.06	-14.86	-14.84	-14.56	-14.27	-14.12	-14.22		-15.19	C	
+50096	1215	-16.05	-14.97	-14.83	-14.78	-14.63	-14.61	-14.36	-14.12	-13.92	-13.90	-14.01	-14.56	C	-13.13
+50096	1251	-15.98	-14.95	-14.79	-14.75	-14.59	-14.55	-14.30	-14.05	-13.86	-13.84			C	
+50260	1054	-15.65	-14.97	-14.45	-14.51	-14.22	-14.24		-14.24	-14.61	-15.20			M7.0	
+50261	1078	-15.77	-14.88	-14.43	-14.48	-14.33	-14.32		-14.42	-14.77	-15.30			M6.0	
+50357	1215			-16.68		-16.37		-15.79	-15.23	-14.85	-14.64	-14.60	-15.22	C	-13.83
+60015	1251	-15.86	-14.80	-14.20	-14.25	-13.90	-13.91	-13.79	-13.84	-14.15	-14.71		-16.25	M7.8	
+60052	1251	-16.01	-14.84	-14.32	-14.35	-14.11	-14.09	-14.00	-13.99	-14.29	-14.82		-16.20	M6.0	
+60092	1215		-15.63	-14.86	-14.84	-14.18	-14.28	-13.94	-13.80	-13.88	-14.11	-14.31	-14.62	M8.6	-13.24
+60169	1054	-16.90	-15.12	-14.53	-14.47	-13.83	-14.05		-13.52	-13.70	-14.05		-14.86	M9.3	
+60184	1054	-16.76	-15.34	-14.76	-14.75	-14.21	-14.35		-14.26	-14.43	-14.91			M8.8	
+60288	1106	-17.40	-15.67	-14.92	-14.88	-14.19	-14.41			-14.38	-14.79	-15.24	-16.00	M9.3	
+60288	1214		-14.85	-14.22	-14.25	-13.92	-14.00	-13.92	-13.98	-14.26	-14.67	-15.10	-15.69	M8.2	-13.64
+60288	1251	-16.37	-14.92	-14.27	-14.29	-13.92	-14.00	-13.90	-13.91	-14.19	-14.62			M8.2	

TABLE 1 (continued)

Star	JD (2440000+)	log F_λ (W $cm^{-2}\mu^{-1}$) .55μ	.78μ	.87μ	.88μ	1.04μ	1.05μ	1.25μ	1.65μ	2.2μ	3.4μ	5.0μ	10.2μ	Spectral Type	log F (W cm^{-2})
+60289	1215	-16.66	-15.42	-14.77	-14.82	-14.41	-14.44	-14.26	-14.31	-14.61	-15.14	-15.53		M7.9	
+60316	1215	-16.22	-14.94	-14.37	-14.41	-14.12	-14.11	-13.97	-13.97	-14.25	-14.78	-15.36	-16.13	M6.0	-13.71
+60334	1251	-17.12	-15.51	-14.89	-14.85	-14.26	-14.42	-14.12	-14.06	-14.20	-14.54		-15.63	M8.9	
+70102	1052	-16.96	-15.41	-14.84	-14.81	-14.28	-14.47		-14.22	-14.49	-14.88		-15.93	M9.0	-13.92*
+70171	1215	-17.64	-15.78	-15.13	-15.05	-14.43	-14.64	-14.18	-14.08	-14.25	-14.63	-15.07	-15.65	M9.2	-13.73
+70171	1251	-17.79	-15.89	-15.25	-15.16	-14.53	-14.75	-14.34	-14.19	-14.35	-14.73		-15.73	M9.3	-13.84*
+80005	1050	-17.97	-16.05	-15.25	-15.17	-14.46	-14.70	-14.20	-14.17	-14.41	-14.87			M9.5	
+80005	1215	-18.18	-15.84	-15.06	-15.05	-14.36	-14.57	-14.06	-14.06	-14.30	-14.76	-15.21	-16.14	M9.2	-13.77
R And	1214	-16.06	-14.44	-13.86	-13.83	-13.41	-13.37	-13.07	-13.06	-13.32	-13.73	-14.14	-14.69		-12.76
R And	1277	-16.87	-15.18	-14.46	-14.47	-13.90	-13.83	-13.58	-13.44	-13.63	-13.96				
W And	1215	-14.89	-13.97	-13.42	-13.45	-13.12	-13.13	-12.99	-13.08	-13.40	-13.91	-14.40	-15.17	M6.5	-12.80
W And	1251	-15.62	-14.30	-13.70	-13.72	-13.27	-13.29	-13.19		-13.46	-13.95			M7.9	
W And	1277	-15.98	-14.58	-13.94	-13.92	-13.39	-13.47	-13.13	-13.20	-13.49	-13.97			M8.3	
W And	1302	-16.30	-14.82	-14.16	-14.12	-13.50	-13.65			-13.46	-13.89			M8.9	
T Aqr	1251	-16.59	-15.29	-14.68	-14.75	-14.44	-14.49	-14.48	-14.61	-14.92	-15.40			M8.0	
T Ari	1214	-14.88	-13.85	-13.30	-13.37	-13.13	-13.13	-13.12	-13.18	-13.53	-14.06	-14.54	-15.51	M7.0	-12.90
U Ari	1251	-17.03	-15.22	-14.44	-14.42	-13.73	-13.98	-13.68	-13.77	-14.06	-14.45			M9.5	
U Ari	1277	-16.79				-13.65	-13.90	-13.67	-13.75	-14.04	-14.46				
R Boo	1078	-16.11	-14.89	-14.20	-14.25	-13.84	-13.91		-13.92	-14.25	-14.74			M8.1	
R Cam	1078	-15.47	-14.39	-14.20	-14.18	-14.12	-14.10		-14.16	-14.54	-15.08				
R Cas	1214	-15.79	-14.10	-13.46	-13.40	-12.77	-13.00	-12.53	-12.54	-12.77	-13.19	-13.62	-14.22	M9.3	-12.22
R Cas	1251	-16.11	-14.32	-13.67	-13.58	-12.87	-13.15	-12.71	-12.68	-12.88	-13.30		-14.49	M9.7	
R Cas	1302	-16.11	-14.38	-13.75	-13.67	-12.90	-13.20			-12.83	-13.18			M9.9	
T Cas	1214	-15.95	-14.28	-13.59	-13.57	-12.98	-13.15	-12.76	-12.78	-13.06	-13.56	-14.05	-14.84	M8.9	-12.52
T Cas	1251	-15.76	-14.14	-13.46	-13.44	-12.87	-13.00	-12.70	-12.76	-13.04	-13.52		-15.01	M8.7	
V Cas	1214	-15.49	-14.36	-13.72	-13.77	-13.40	-13.43	-13.32	-13.40	-13.73	-14.24	-14.79	-15.73	M7.9	-13.13
Y Cas	1214	-15.46	-14.23	-13.72	-13.74	-13.41	-13.48	-13.41	-13.47	-13.74	-14.18	-14.63	-15.29	M8.1	-13.13
SS Cas	1277	-14.91	-14.39	-14.18	-14.20	-14.20	-14.18	-14.24	-14.36	-14.69	-15.18			M4.0	
T Cep	1214	-15.06	-13.68	-13.01	-13.02	-12.47	-12.60	-12.36	-12.43	-12.75	-13.26			M8.6	
R Cyg	1214	-14.72	-13.65	-13.47	-13.45	-13.35	-13.35	-13.31	-13.41	-13.74	-14.18				
χ Cyg	1214	-15.35	-13.61	-12.74	-12.82	-12.34	-12.41	-12.29	-12.39	-12.65	-13.05			M8.2	
S Lac	1251	-16.29	-15.09	-14.50	-14.51	-14.04	-14.11	-13.96	-14.06	-14.35	-14.86		-16.42	M8.2	-13.77*
R Leo	1109								-11.76	-11.12	-12.58	-13.17	-14.00		
W Lyr	1214	-15.74	-14.88	-14.40	-14.46	-14.28	-14.29	-14.30	-14.40	-14.73	-15.21			M6.5	
V Mon	1277	-14.54	-13.71	-13.35	-13.38	-13.25	-13.24	-13.22	-13.30	-13.65	-14.16			M5.0	
R Tri	1214	-13.99	-13.47	-13.22	-13.25	-13.21	-13.21	-13.28	-13.38	-13.76	-14.26	-14.67	-15.63	M5.0	-13.03
R Tri	1251	-14.30	-13.60	-13.23	-13.27	-13.17	-13.17	-13.21	-13.30	-13.67	-14.19			M5.5	
R Tri	1277	-14.87	-13.97	-13.41	-13.47	-13.23	-13.23	-13.21	-13.32	-13.66	-14.18			M7.0	
W Peg	1214	-15.93	-14.45	-13.87	-13.83	-13.28	-13.44	-13.08	-13.12	-13.39	-13.87	-14.36	-15.14	M8.9	-12.84
Z Peg	1214	-16.28	-14.84	-14.20	-14.19	-13.70	-13.80	-13.48	-13.57	-13.85	-14.34	-14.96	-15.80	M8.5	-13.30

*Total flux computed by assuming $F_{5\mu}$ given by black-body fit to shorter wavelength infrared data.

determination of continuum colors with respect to the longer infrared wavelengths. Observations of Miras on the near-infrared system were published by Lockwood (1972) along with the derivation and calibration of the photometric spectral types. A recent modification of the technique for determining spectral types of stars later than M7.5 is discussed in Wing and Lockwood (1973) and Lockwood (1973).

We have listed the observational data for Mira variables and IRC stars in table 1 along with the star name or IRC number and the mean Julian Date of the observations. The data were obtained nearly simultaneously, being restricted to an interval of 10 days or less in order to minimize the effects of variability upon the interpretation. This is especially important with regard to the data shortward of 1 μ where the colors and spectral types of these cool stars often change very rapidly (*cf.* Lockwood and Wing 1971).

Note that we depart from convention in choosing to present the data only in units of log flux (W cm^{-2} μ^{-1}) rather than in magnitudes; this has been done in order to avoid the confusion presented by the two photometric systems which have different definitions for the colors of standard stars. Clearly this form has a much sounder physical basis as well. The absolute calibration at 0.55 μ and from 1.25 to 10.2 μ is taken from Johnson (1966) except at 1.65 μ where we have adopted 1.18 $\times$ 10^{-13} W cm^{-2} μ^{-1} for the flux corresponding to mag = 0.0. The near-infrared data were first transformed to the absolute scale of Hayes (1970) and then to absolute flux using the adopted zero-point at 1.04 μ of 5.65 $\times$ 10^{-13} W cm^{-2} μ^{-1} for mag = 0.0. We define F_λ to be the monochromatic flux in W cm^{-2} μ^{-1} at wavelength λ and $\mathscr{F} = \int F_\lambda d\lambda$ to be the total flux in W cm^{-2} where the integration is taken using the trapezoidal rule over the significant part of the energy distribution. For computing the total fluxes, which are listed in table 1, we have required (except for the six cases noted in the table) that all infrared colors be present. For five IRC stars, there was no 1.25- or 5-μ observation, but a 5-μ flux was estimated by taking the blackbody value predicted by fitting the other data points. For S Lac, the 1.25-μ point exists, but it was necessary to estimate a 5-μ flux by the same procedure. We felt that the addition of this material to the whole was sufficient to justify the uncertainties introduced by the technique for reasons that will become apparent in § V.

Internal errors in the observational data depend upon the spectral region: In general the photoelectric data at $\lambda \leq 1.05$ μ are good to 2–3 percent except at 0.55 μ where many of the IRC stars are extremely faint. In the 1–4-μ region, the errors should be 5 percent or less and at 5 and 10.2 μ about 10 percent or slightly greater. These are insignificant for the purposes of this paper when compared with the errors of the absolute calibration which may be as great as 10 percent at each wavelength (Johnson 1965*b*) and which therefore dominate the errors in determining such quantities as color-temperature and total flux. Photometric spectral types as determined here are inherently of high accuracy because of the precision with which molecular-band strengths can be measured; errors in these are therefore of no consequence for the purposes of this paper.

III. PHOTOMETRIC PROPERTIES

One of the principal aims of this paper is to try to determine which are normal among the sample of coolest stars. In order to define such a subset, one must assess the contribution to the observed flux by circumstellar shells. Basic characteristics of the infrared energy distributions of cool stars have been previously discussed in the literature, for example, by Johnson (1966), Gehrz and Woolf (1971), Gillett, Merrill, and Stein (1971), and Hyland *et al.* (1972). Many stars have been found to have infrared excesses within the range of spectral types from M0 to M6 based upon a comparison of the infrared colors to that expected from a Rayleigh-Jeans distribution. The problem here is to construct an adequate definition for infrared excess within the entire range from M0 to M10. We might expect *a priori* that the Rayleigh-Jeans approximation would not be adequate and search for an alternative. A better approximation would be simply to compute the blackbody colors as a function of temperature. The temperature, however, is one of the quantities we ultimately seek to derive from the data and hence we cannot proceed in an entirely satisfactory manner. Alternatively, the infrared colors of a blackbody are not strong functions of the temperature within the expected range (2000°–4000° K) and it should be possible to make a good first guess.

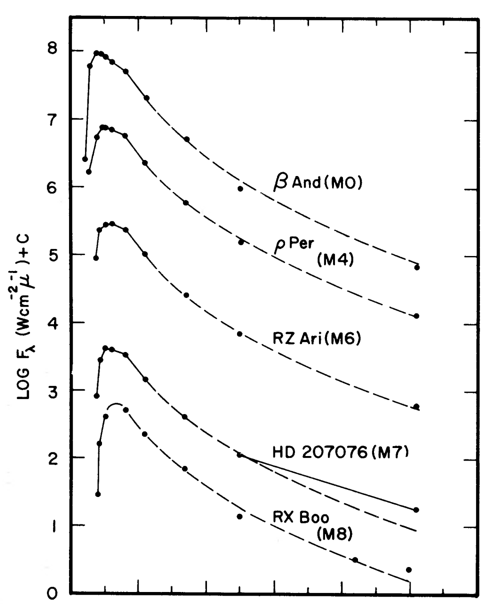

FIG. 1.—Energy distributions for some normal giant stars from M0–M8. Blackbody colors (*dashed lines*) have been fitted to the data at 2.2 μ using T = 4000° K for β And and T = 3000° K for the other four stars.

In figure 1, we have shown a sample of energy distributions for some normal giants where the data have mostly been taken from Lockwood (1972), Johnson *et al.* (1966), Gillett *et al.* (1971), and Gehrz and Woolf (1971) with some supplementary unpublished data taken at Kitt Peak. For reference, we have shown blackbody colors normalized at 2.2 μ using a temperature of 4000° K for β And (M0) and 3000° K for the other four stars (M4 through M8). Several important points should be noted. First, the adopted blackbodies give a reasonable representation of the infrared colors and only HD 207076 (M7) shows a significant indication of an infrared excess. In particular, it is interesting that $T = 3000°$ K is satisfactory over the entire range from M4–M8. Second, note that the peak in the flux curve shifts to longer wavelengths with advancing spectral type indicating the decline in temperature. The opacity window at 1.65 μ clearly shows as a bump longward of the flux maximum. In the coolest M stars, the thermal maximum combines with the opacity minimum to produce a strongly peaked distribution.

Clearly, a smooth progression in color exists for the stars in figure 1 and one might be led to expect an orderly extension to later types. However, it is well-known that the likelihood of stars having circumstellar shells increases among the giants with decreasing temperature. In figure 2, we have shown a sequence of energy distributions for a sample of IRC stars within a restricted range of spectral type (and therefore temperature) which are compared to the infrared colors of a 2000° K blackbody normalized at 2.2 μ. These are all high-latitude stars ($|b^{\mathrm{II}}| \geq 15°$) so that effects of *interstellar* reddening are likely to be negligible. Thus, one can see empirically the effects of circumstellar shells upon the observed energy distributions. For IRC+80005 we would say that there is no obviously observable indication of a shell of dust. As one proceeds upwards in the figure, one notes first an excess at 10.2 μ and then excesses at progressively shorter wavelengths until, for +40004, attaching a blackbody at 2.2 μ has no meaning. Note how the shape of the energy distribution between 1 and 2 μ is affected as the shell emission becomes more and more prominent at longer wavelengths. Whether the deformation in the distribution is caused primarily by shell emission or by shell reddening is impossible to determine without detailed models, although one would certainly expect some combination of the two. If the emitting material is similar in all the shells as one might expect for M stars (Gehrz and Woolf 1971; Gillett *et al.* 1971), and if the shell temperatures are similar, then the optical thickness at 10.2 μ must increase as the observed ratio $F_{10.2\,\mu}/F_{2.2\,\mu}$ increases. One can see that for the three uppermost stars the shell temperatures are similar since the ratio $F_{10.2\,\mu}/F_{5\,\mu}$ remains nearly constant and is primarily representative of the shell flux for those stars, again assuming the same material for each of those three stars. Thus, we believe that the sequence shown in figure 2 fundamentally represents one in which the shell optical thickness increases as one moves upward in the figure.

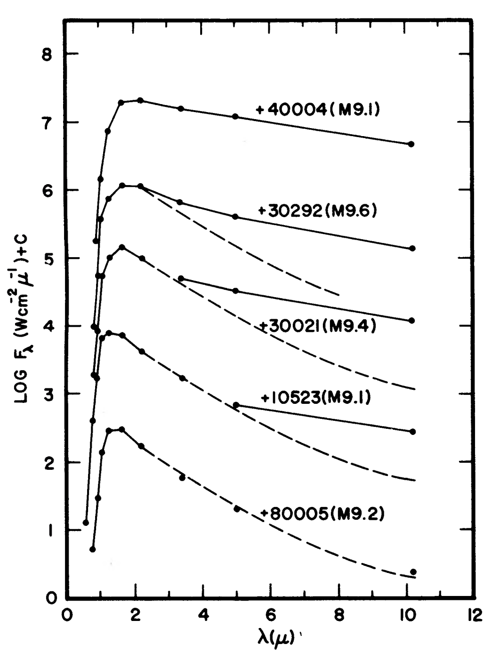

FIG. 2.—Energy distributions for IRC stars at high galactic latitude selected within a restricted range of spectral types (M9.1–M9.6) with a 2000° K blackbody (*dashed line*) normalized to 2.2 μ. Note the effect of circumstellar shell emission upon the energy distribution as the excess at 10.2 μ increases.

Figure 2 illustrates that the colors shortward of 5 μ are probably reasonably uncontaminated for +10523 even though the excess at 10.2 μ is a factor of 6 above that expected on the basis of blackbody colors. For the purpose of future discussion in this paper, we will define a star as "normal" in terms of its colors at wavelengths shorter than 5 μ if the excess at 10.2 μ is ≤ 4 times the expected blackbody flux. We will adopt blackbodies of $T = 4000°$ K for types M0–M4, $T = 3000°$ K for M4–M7.9, $T = 2500°$ K for M8–M8.9, and $T = 2000°$ K for M9–M10 as the grid of normal infrared colors for those spectral intervals, based upon inspection of figures 1 and 2.

Before ending the discussion of photometric properties of the IRC stars, it is instructive to consider the energy distributions of four extraordinarily red carbon stars shown in the lower panel of figure 3. We have also shown the energy distribution of NML Cyg (classified as an M-type star by Herbig and Zappala 1970) for comparison in the upper panel. In general these extreme carbon stars have energy distributions characterized by maxima occurring longward of 2 μ in comparison to those of the M-type stars which peak near 1.6 μ or shortward. Interstellar reddening doubtless plays a role in shaping the observed fluxes, but is probably not the dominant factor since the second reddest star (−10236) is a high-latitude star ($b^{\mathrm{II}} = 34°$).

It has previously been noted by Strecker, Ney, and Murdock (1973) that the gross energy distributions for some of the IRC carbon stars resemble that of

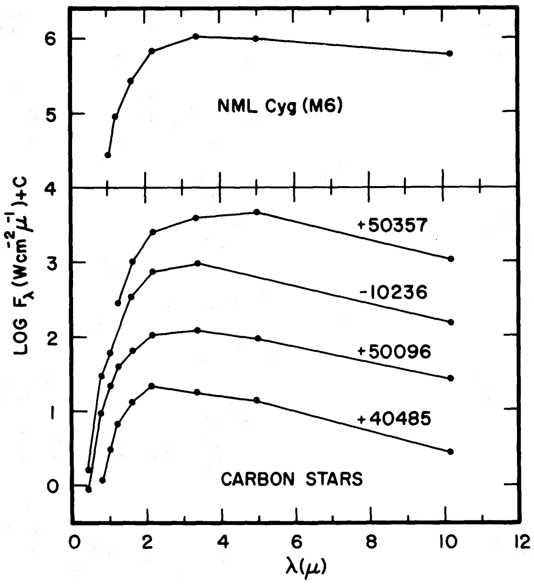

FIG. 3.—A comparison between energy distributions for NML Cyg (M6) and for three very red carbon stars. Note the gross similarity in the character of the distributions even though the stars themselves are quite different.

NML Cyg. This is clearly apparent in figure 3 which demonstrates that a classification scheme based only upon the broad-band photometry can be misleading.

IV. TEMPERATURES

Historically, the determination of stellar temperature has been a subject of great interest. For cool stars, the temperature scales have always been troublesome because of the poor correspondence between most kinds of observationally determined color temperatures and the effective temperatures, the large amount of flux radiated in the infrared, the totally inadequate representation of the observed energy distributions by blackbody curves, and the unavailability of theoretical models. In this section, we will use our data to derive a relation between color temperature and spectral type which appears to be valid for the latest M stars, and will reexamine the fundamental effective temperature scale for cool stars.

a) The Relation between Color Temperature and Spectral Type

In Johnson's (1966) review of infrared measurements, it was pointed out that the $I - L$ color temperature gave the best estimate of effective temperature for stars of all spectral types down to about M6, although the scatter for the six M stars with known effective temperatures was extremely large. In the spectral range of interest to us (i.e., later than M6) Johnson gave only temperatures derived from blackbody fits to the observed energy distributions of a few very cool stars such as NML Tau[1] and NML Cyg.

[1] NML Tau = IRC+10050 now has the variable star designation IK Tau.

Since both of these stars have energy distributions which are strongly affected by the presence of circumstellar shells (Neugebauer, Becklin, and Hyland 1971) and by interstellar reddening for NML Cyg, the temperature scale determined from them will be dependent upon an unknown amount of reddening and/or emission.

Inspection of the 27-color (0.75–1.08 μ) scans of M6–M10 stars given by Wing (1967) reveals that the broad-band I passband of the Johnson photometric system is seriously affected by TiO, VO, and H_2O absorption; in fact, the scanner data shows that there are no regions of uncontaminated continuum shortward of 1.04 μ in these stars. By folding the I filter response function (Johnson 1965*a*) into the observed scans, we were able to estimate that the observed flux at I will be too low by a factor of 2 at M6–M8 and by a factor of 5 at M10, with respect to the flux expected by fitting a blackbody to the 1.04- and 3.4-μ points. In other words, Johnson's color temperature, which uses the same long-wavelength color as ours but a different short-wavelength one, is much more sensitive to the vagaries of blanketing and hence is unsuitable for use with the coolest stars. We have therefore adopted a color temperature based upon the ratio $F_{1.04\,\mu}/F_{3.4\,\mu}$.

In order to choose a sample of "normal" stars, we have applied the criteria outlined in § III for minimizing the influence of circumstellar shells upon the intrinsic colors of the underlying star. In addition, we have restricted the sample to stars at galactic latitudes $|b^{\rm II}| \geq 15°$ which are, presumably, free of serious interstellar reddening at 1.04 μ. The sample of IRC stars and Mira variables chosen has been listed in table 2 where we have given the color temperature, T_c, from fitting blackbody colors to the fluxes at 1.04 and 3.5 μ. In addition, we have tabulated data for some normal giants which meet our criteria for minimizing interstellar and circumstellar reddening. The data for this latter group have been taken from Lockwood (1972), Gehrz and Woolf (1971), Gillett *et al.* (1971), and Johnson *et al.* (1966) and supplemented with a few of our unpublished data. In order to illustrate the relation between T_c and photometric spectral type, we have plotted the data from the table in figure 4. We can see that an excellent relation exists over the range from M0–M10 and that there are apparently no systematic differences in the relationship for IRC stars, Miras, and giants even though they exhibit diverse variability characteristics. In that relation, note the precipitous decrease of the ratio after M6—between M6 and M10 it changes by a factor of 10 indicating that the flux ratio is a remarkably sensitive indicator of color temperature over this range. By comparing the mean values at each spectral type for which there is more than one observation, we find that the *average* deviation from the mean over the entire range is approximately 75° K. This scatter is to be compared with the estimates of the observational error in both coordinates shown at three points in figure 4, where we have estimated that the measurement error in $F_{1.04\,\mu}/F_{3.4\,\mu}$ is 10 percent. Clearly, the observational errors can account for

TABLE 2

SUMMARY OF SOME DERIVED PHYSICAL QUANTITIES

Star	b^{II}	JD 2,440,000+	Spectral Type	T_c (° K)	log $F_{2.2\,\mu}/\mathscr{F}$	log $F_{1.04\,\mu}/\mathscr{F}$	log $F_{0.55\,\mu}/\mathscr{F}$	Notes
IRC Stars and Mira Variables from This Program								
−30217	+30	1050	M9.8	2042	−0.55	−0.45	−3.73	1, 2
−20293	+26	1051	M7.9	2365	−0.56	−0.34	−2.50	1, 2
+00028	−55	1215	M7.9	2588	−0.58	−0.27	−2.21	...
+00266	+46	1050	M9.6	1774	−0.48	−0.67	−3.99	1, 2
+20052	−32	1215	M8.1	2290	−0.55	−0.40	−2.67	...
+20328	+24	1106	M9.8	1850	...	...	...	MW Her
+30055	−25	1215	M7.9	2329	−0.57	−0.39	−2.62	...
+30515	−28	1215	M7.9	2510	−0.58	−0.32	−2.36	...
+70102	+43	1052	M9.0	2191	−0.57	−0.36	−3.04	...
+70171	+15	1215	M9.2	1790	−0.52	−0.70	−3.90	...
+70171	+15	1251	M9.3	1796	−0.51	−0.69	−3.95	2
+80005	+17	1215	M9.2	1967	−0.53	−0.59	−4.41	...
T Ari	−37	1214	M7.0	2689	−0.63	−0.23	−1.98	...
S Lac	−15	1251	M8.2	2502	−0.59	−0.28	−2.53	2
R Tri	−33	1214	M5.0	2960	−0.72	−0.18	−0.95	...
W Peg	−32	1214	M8.9	2175	−0.55	−0.44	−3.09	...
Z Peg	−36	1214	M8.5	2239	−0.56	−0.41	−2.98	...
Supplemental Data for Some Normal Giants								
β And	−27	...	M0	3450	−0.80	−0.18	−0.32	...
75 Leo	+56	...	M0	3400	−0.79	−0.22	−0.33	...
α Cet	−46	...	M1	3300	−0.81	−0.24	−0.49	...
83 UMa	+61	...	M2	3250	−0.80	−0.24	−0.50	...
χ Peg	−42	...	M2	3350	−0.81	−0.24	−0.48	...
β Peg	−29	...	M3	3250	−0.73	−0.19	−0.58	...
ρ Per	−17	...	M4.0	3100	−0.71	−0.19	−0.83	...
RR UMi	+47	...	M4.5	3300	−0.65	−0.16	−0.86	...
BS 5299	+67	...	M4.5	3050	−0.68	−0.20	−0.94	...
AC Dra	+18	...	M4.5	3100	−0.65	−0.15	...	...
R Lyr	+18	...	M5.0	3050	−0.65	−0.20	−1.08	...
RZ Ari	−35	...	M6.0	2950	−0.63	−0.20	...	...
g Her	+44	...	M6.0	2950	−0.63	−0.18	−1.53	...
τ^4 Ser	+51	...	M6.5	2700	−0.62	−0.24	...	...
HD 207076	−38	...	M7.0	2900	−0.59	−0.14	...	...
RX Boo	+69	...	M8.0	2400	−0.58	−0.33	...	...

NOTES.—(1) No flux at 1.25 μ. (2) Flux at 5 μ estimated from infrared blackbody colors.

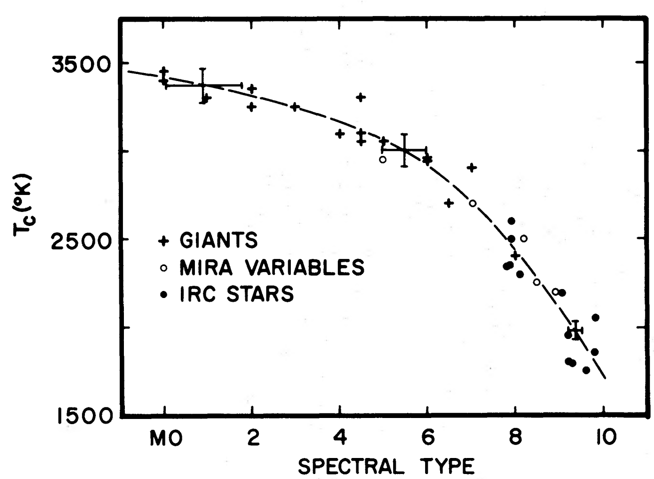

FIG. 4.—The relationship between the color temperature, T_c, determined from blackbody fits to the flux ratio $F_{1.04\,\mu}/F_{3.4\,\mu}$ and photometric spectral type. The stars shown here are at high galactic latitude and have been selected to minimize the effects of circumstellar shells upon the energy distributions. Representative observational error bars are shown at three points in the diagram.

the scatter from M0 to about M7, but beyond that the scatter is larger than the estimated error. Many of the cooler IRC stars are undoubtedly Miras; we believe that the scatter at the later types is real and is related to the variations in color temperature at a given band strength that have been observed in the cyclical variations of Miras (Wing 1967; Lockwood 1972). Also, for the cooler stars, 1.04 μ is well to the blue side of the flux maximum making the flux at 1.04 μ exponentially dependent on temperature.

b) *Effective Temperatures*

The recent availability of stellar diameters for cool giants measured by speckle interferometry (Gezari, Labeyrie, and Stachnik 1972; Bonneau and Labeyrie 1973) and for the Mira star R Leo at an advanced phase by lunar occultation (Nather and Wild 1973) have made possible a reexamination of the effective temperature scale for these stars. The speckle interferometric diameters are in good agreement with the ones determined with the Michelson interferometer 40 years earlier (Pease 1931), so that no radical changes in the effective temperature scale were suspected from this source. However, the availability of a diameter for a star as cool as R Leo is a highly significant new datum.

It is worthwhile to discuss the various errors which are important in the calculation of effective temperatures. We can compute the formal error in the effective temperature arising from observational errors in the total flux and the angular diameter by assuming that the error is governed by propagation theory. Thus, the relative error in the effective temperature is

$$\frac{\epsilon_{T_e}}{T_e} = \frac{1}{2}\left[\left(\frac{\epsilon_\theta}{\theta}\right)^2 + \frac{1}{4}\left(\frac{\epsilon_{\mathscr{F}}}{\mathscr{F}}\right)^2\right]^{1/2},$$

where θ is the angular diameter of the star and ϵ_θ, $\epsilon_{\mathscr{F}}$ are the errors in θ and $\mathscr{F}$, respectively. Errors in the absolute calibration of the flux from Vega are estimated by Johnson (1965*b*) to be of the order of 10 percent or less. For stars as bright as those which have effective temperature data, the main source of error in the total flux will in fact be the uncertainty in the absolute calibration since, as we have previously discussed, the flux *relative* to Vega is very well determined and the color of Vega is likewise well determined. To take an example, the quoted formal uncertainty in the angular diameter of α Boo is 14 percent (Gezari *et al.* 1972) and hence the relative error in T_e is 7 percent, or approximately 300° K. Typically, the relative errors in the angular diameters are of the same order as that for α Boo so that the major contribution to the observational error in T_e will result from that source.

An important source of systematic error which cannot be accurately assessed is the error introduced into the total flux by ignoring the detailed structure of the energy distributions both inside and outside the atmospheric transparency windows. In an attempt to set an upper limit on the error in the total observed flux, we have examined scans of the cool M stars α Her (M5 Ib–II) and RX Boo (M8e) from 1 to 10 μ made by Ridgway (1973) at Kitt Peak using a Fourier transform spectrometer. In these scans about 25 percent of the stellar flux is not recorded because of telluric absorption bands. Inspection of the shapes of the stellar absorption bands visible outside the telluric bands, however, suggests that a reasonable value for the total stellar molecular absorption is ~10 percent for α Her and ~15 percent for RX Boo. In neither case could the absorption be as much as twice these values; hence it appears that we are not overestimating T_e, which goes as the fourth root of the flux, by more than a few percent because of this uncertainty.

We conclude that the observational errors in T_e will be dominated by errors in the angular diameters and may be as large as ±7 percent. Further, a small systematic error (~2–4 percent) at the latest types will produce a scale error in our calibration of T_e. It seems unlikely that the actual errors in the T_e scale could be significantly larger than these values.

A summary of our results for seven K and M stars is presented in table 3. Again, the fluxes have been taken from many sources in the literature which have been noted previously. The photometry of o Cet was obtained near the 1966 maximum nearly simultaneously by Wing (1967) and by Mendoza (1967) at the same phase at which the angular diameter was measured by Bonneau and Labeyrie (1973); the spectral type determined by Wing was M5.5. The photometric spectral type M8.4 for R Leo was determined by

TABLE 3

CALIBRATION OF THE SCALE FOR COLOR TEMPERATURE VERSUS EFFECTIVE TEMPERATURE

Star	Spectral Type	Angular Diameter	Total Flux (W cm^{-2})	T_c(° K)	T_e(° K)
α Boo......	K2 III	0\".022	5.22×10^{-12}	3850	4200
α Sco......	M2	0.042	6.82×10^{-12}	3150	3250
α Ori......	M3	0.052*	1.04×10^{-11}	3200	3250
β Peg......	M3	0.016	1.61×10^{-12}	3250	3650
o Cet......	M5.5:	0.051†	3.15×10^{-12}	2250	2450
α Her......	M5.5	0.031	4.15×10^{-12}	2950	3350
R Leo.....	M8.4	0.067	2.75×10^{-12}	2250	2050

* Adopted diameter at 7190 Å.

† Adopted diameter at 7500 Å for JD 2,441,474.

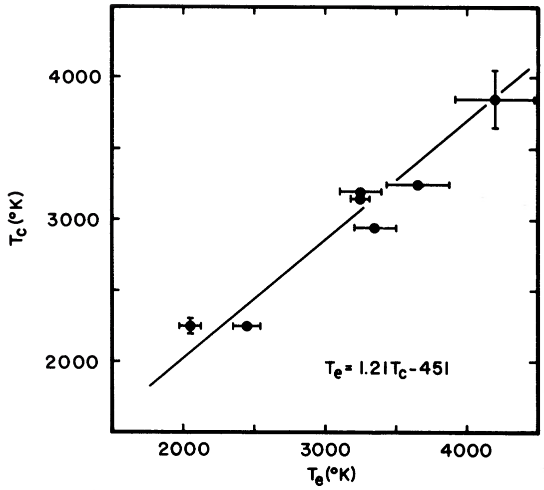

FIG. 5.—The relation between the color temperature (T_c) and the effective temperature (T_e) for the seven stars having speckle interferometric or lunar-occultation angular diameters. The line is the result of a least-squares fit to the data yielding the equation shown in the lower right corner of the figure.

Lockwood (unpublished) one day after Nather and Wild's (1973) observation of the diameter. Unfortunately, no data longward of 1 μ were obtained at Kitt Peak for that date, so we have used data for the same phase in the previous cycle, when the spectral type was also M8.4 but when the flux at 1.04 μ was twice as great. It is difficult to estimate the error in the derived T_e for R Leo from this source, but it is hard to imagine how it could exceed 20 percent. In any case, this is by far the coolest star for which a determination of T_e has ever been possible, however imprecise. Included also in table 3 are the observed diameters and our color temperatures.

In figure 5 we have illustrated the relationship between T_c and T_e for the stars in table 3. We have fitted a line through the data by the method of least squares which results in the relationship

$$T_e = 1.21T_c - 451 .$$

Formal errors in T_e arising from the errors of measurement of the diameters and total flux as discussed above have been shown in the figure, as well as representative error bars for T_c arising from an estimated error of 10 percent in the flux ratio. The errors are, of course, much more important in an absolute sense at higher temperatures. We have not considered in this relation the possible overestimate of T_e resulting from the overestimate of the total flux caused by ignoring the stellar H_2O opacity. The general character of the relation would still exist, namely that the color temperature underestimates the effective temperature at 4000° K, but overestimates it at 2000° K. Some curvature to the relation would perhaps be added if the water opacity were taken into account.

In comparing our effective temperature scale with Johnson's (1966) earlier one, we find good agreement in the mean relation which would have resulted from using our color temperature and his effective temperatures. However, the individual values of T_e do not always agree. Furthermore, our temperature scale for stars cooler than 3000° K is several hundred degrees higher than his; this is a larger difference than can be accounted for by water-vapor opacity, which Johnson attempted to correct for using Stratoscope data.

V. TOTAL FLUXES AND OTHER DERIVED QUANTITIES

a) Fluxes

We have also listed log $F_{0.55\,\mu}/\mathscr{F}$, log $F_{1.04\,\mu}/\mathscr{F}$, and log $F_{2.2\,\mu}/\mathscr{F}$ in table 2. It should be noted that the total fluxes listed in table 1 are related to the classical "bolometric magnitude" by the relation $m_{\text{bol}} = -2.5 \log \mathscr{F} - 28.87$, where the additive constant is derived from the observed visual magnitude and total flux for the Sun such that the Sun has $m_{\text{bol}} - V = 0.0$. Estimates of the ratio of the flux at 0.55 μ to the total flux have been made for M stars by Smak (1966) and others. These bolometric corrections are highly uncertain because of serious blanketing effects of TiO on the visual spectrum and because of the extreme sensitivity upon the spectral types. As the energy distributions in § III amply demonstrate, a much better idea of the total flux of an M star can be obtained from measuring either $F_{1.04\,\mu}$ or $F_{2.2\,\mu}$ both of which are

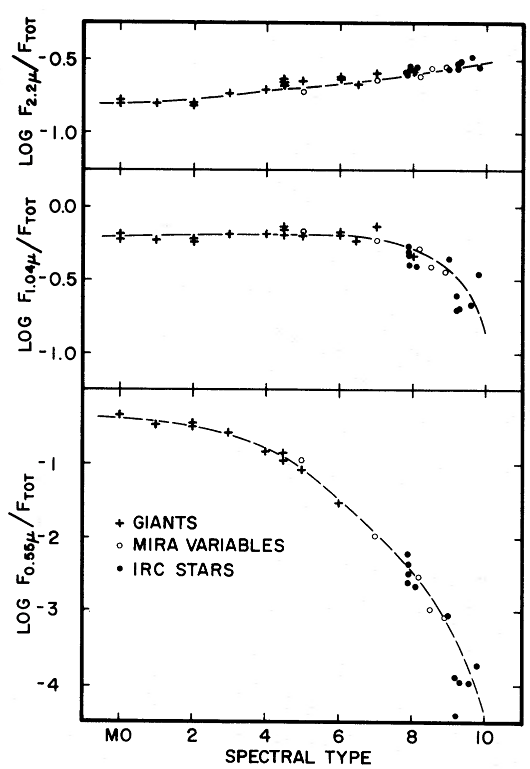

FIG. 6.—The relations between spectral type and the ratios of fluxes at 2.2, 1.04, and 0.55 μ to the total flux. Note that the relation at 1.04 μ is extremely flat out to M7 and that at 2.2 μ the ratio changes very slowly over the entire range M0–M10.

easily measurable and many values of which have been published in the literature in the form of $I(104)$ or K-magnitudes. Observations at 1.25 or 1.65 μ would also probably be suitable.

In figure 6, we present plots of the log of the ratio of the monochromatic flux at 2.2, 1.04, and 0.55 μ to the total flux as a function of photometric spectral type for all of the stars in table 2. As previously noted for the relationship between T_c and spectral type, there seems to be no systematic differences among the sample of IRC stars, Miras, and giants. Furthermore, the scatter for the 2.2-μ data is extremely low. Most notable in our judgment is the extremely flat relationship for the 2.2-μ data all the way from M0 to M10. A consequence is that if a star is simply known to be of type M, with no indication of subtype, the total flux can be obtained within a factor of 2 from the K-magnitude alone. By comparison, the relation for 104 μ is somewhat flatter for stars earlier than M6, but falls off rapidly after M8, although the scatter in the data prevents an accurate determination of the relationship in this spectral region. Fortunately, the vast majority of known M stars are earlier than M8, which means that a simple measurement of $I(104)$ can predict the total flux to within about 10 percent. As expected, the relation for the 0.55-μ data is extremely steep and relatively noisy, changing by a factor of 10^4 from M0 to M10, and is included here simply for comparative illustration. Note that a misclassification of one subtype at M9 means an error in the correction to the 0.55-μ flux of more than a factor of 10.

b) *Angular Diameters*

Given the total fluxes and extrapolating the effective temperatures to the latest types via the relation between spectral type and color temperature, we can estimate angular diameters for some of the brighter stars on our program. There are eight IRC stars and two Mira variables for which we have the total flux and which are bright enough to make the calculations worthwhile. The results are, unfortunately, disappointing. For −30217, +10523, +30021, +30515, +60092, +70102, and +70171, the values lie within the range $0''.004 \leq \theta \leq 0''.008$; for NML Cyg (+40448) $\theta \simeq 0''.01$ if no allowance is made for reddening. The Miras R Cas and W Peg should have, respectively, angular diameters of 0″.03 and 0″.02. For NML Tau we do not have the total flux but we can estimate it from the 2.2-μ flux and the correction from figure 6 for the spectral type M9.5; we find that $\theta = 0''.03$. Thus, we have the results that the stars which would be best suited to tie down the effective temperature scale at the low end are sufficiently far away to make the angular-diameter measurement nearly impossible with present techniques. Only R Cas and NML Tau offer any hope among the sample of stars measured here.

c) *Circumstellar Shells*

An interesting question to consider is the frequency of circumstellar shells among the cooler stars. In figure 7 we have shown a plot of $\log F_{10.2\,\mu}/F_{2.2\,\mu}$ versus spectral type with the corresponding effective temperature scale at the bottom for some of our program stars and some normal giants. The plot includes all M-type program stars for which we have the necessary infrared data and as before, the photometry and spectral types for the giants have been taken from sources previously mentioned. Also shown as a line is the flux ratio for blackbodies appropriate to the effective temperature at each spectral type. Note that the line falls above the observed points for the hotter stars and below for the cooler ones. This behavior is expected on the basis of earlier experience. For example, β And, an M0 star shown in figure 1, has been fitted in the infrared with a 4000° K blackbody whereas the effective temperature is about 3700° K. Presumably this relationship between effective and infrared color temperature for the hotter stars is caused by the effect of free-free absorption by H^-, the dominant source of continuous opacity in the infrared for these stars. The free-free absorption increases toward longer wavelengths so that one sees to higher levels in the atmosphere and hence to cooler temperatures. Thus, the flux would fall faster to longer wavelengths than, say, a blackbody of 3500° K, imitating the behavior of a hotter blackbody. For the later spectral types, we would not expect to observe that behavior since the dominant source of opacity would be molecular blanketing.

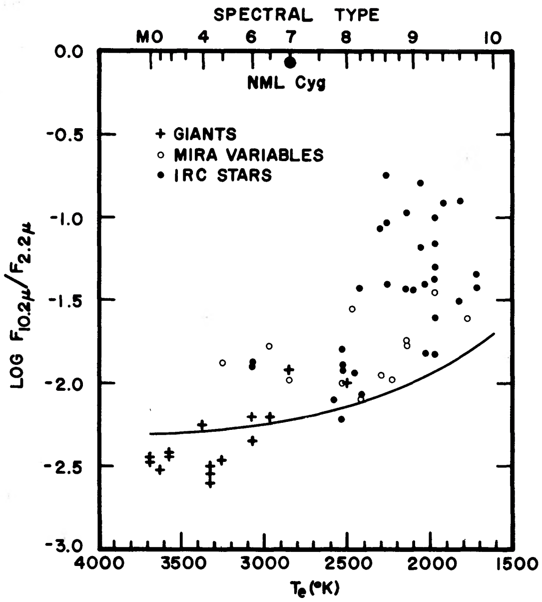

FIG. 7.—The relationship between the ratio of 10.2- and 2.2-μ fluxes and spectral type with the corresponding T_e scale shown at the bottom. The line represents the ratio expected for blackbodies appropriate to the effective temperature. The departure above the line at the cooler temperatures is taken to be representative of infrared emission from circumstellar dust (see text for discussion).

In spite of this apparently systematic problem with the precise definition of the intrinsic colors, we feel that it is important to note that the rise in the log of the flux ratio is faster than can be accounted for entirely by decreasing temperature. Another way of looking at the data is to define an upper and a lower envelope (excluding NML Cyg); in this picture the upper envelope diverges from the lower envelope as the temperature decreases. Thus, it appears that there is observational evidence of a general trend for the infrared excess to increase with declining T_e. The obvious interpretation to apply to this phenomenon is that, at the lower temperatures, conditions become more favorable for producing dust in the vicinity of the stars. A second noteworthy feature of the figure is also evident: within the range $-2.5 \leq \log F_{10.2\,\mu}/F_{2.2\,\mu} \leq -1.5$ there are 11 Miras and 13 IRC stars; at values higher than -1.5, there is only one Mira but 20 IRC stars. Thus, the IRC stars show predominantly larger infrared excesses than do the Miras within the same range of spectral type. Under the assumptions that the shell temperatures and dust compositions are roughly constant within our sample of stars, the IRC stars have shells with larger optical thicknesses than do the Mira variables.

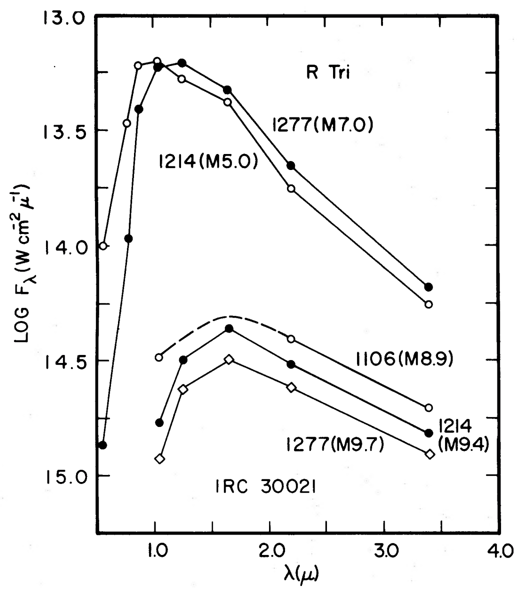

FIG. 8.—Variations in the flux for R Tri, atypical of the sample, and for +30021 which is more representative of the observed variations in IRC stars and Mira variables. The remarkable change shown for R Tri arises because the radius increases sufficiently to overcome the decrease in temperature as the star goes from M5 to M7.

VI. VARIABILITY

Among the IRC stars, a number are known to be periodic variables which have light curves similar in character to the Mira variables. Examples are IRC+10216 (Becklin *et al.* 1969) with a period of approximately 600 days and an amplitude at 1.04 μ of $\Delta \log F_{1.04\,\mu} = 0.6$ (see Zellner and Serkowski 1972) and NML Tau with a period of 470 days and $\Delta \log F_{1.04\,\mu} = 1.1$ (Wing and Lockwood 1973). These 1.04-μ amplitudes are to be compared with typical values of 0.4 for the Mira variables (Lockwood and Wing 1971). At 2.2 μ the amplitude for +10216 and NML Tau are approximately 1.0 and 0.4, respectively. For some other infrared stars, Hyland *et al.* (1972) give 2.2-μ light curves showing roughly similar characteristics. Hence, one might not be surprised if the IRC stars generally show Mira-like variability with longer periods. Indeed, some additional unpublished 1.04-μ data to be discussed later by Lockwood show that +30021 has a period of about 550 days and an amplitude of $\Delta \log F_{1.04\,\mu} \simeq 1.0$ and that +80005 has a period of about 485 days with an amplitude $\Delta \log F_{1.04\,\mu} \simeq 0.7$. In addition, some of our unpublished 2.2-μ data for +30292 coupled with observations kindly supplied to us in advance of publication by E. P. Ney and D. W. Strecker show $P \simeq 475$ days and $\Delta \log F_{2.2\,\mu} \simeq 0.4$. NML Cyg, on the other hand, has shown no convincing evidence for variability (Hyland *et al.* 1972) although it is fair to point out that such stars are indeed rare.

Table 1 does not contain exhaustive information about the infrared variability of the IRC stars. It is possible, however, to make a few comments about the more interesting features of the data at hand. If we restrict the discussion to the 1–4-μ spectral region, the following can be said:

1) A change of flux at one wavelength is *generally* accompanied by a change of flux of the same sign at all other wavelengths. The exceptions are +60288 and R Tri. Comparing JD 2,441,214 and 2,441,277 for R Tri shows that the flux at 1.04 μ changed in the opposite sense to that at 1.25–3.4 μ. The effect was noted in an earlier cycle by Wing (1967). Between JD 2,441,214 and 2,441,251, +60288 showed no change at 1.04 μ, but an increase from 1.25–3.4 μ. In figure 8 we have shown data for R Tri, as an example of unusual behavior for our sample of stars, and for +30021 which is more nearly representative of the sample.

2) A decrease in the 1–4-μ flux in the M stars is usually accompanied by an increase in spectral type (a decrease in T_e) and vice versa. The exceptions, again, are R Tri which shows a change from M5 to M7, but an increase in the 1.25–3.4-μ flux and +60288 (comparing JD 2,441,214 and 2,441,251) which shows an increase in 1.25–3.4-μ flux, but no change in spectral type. For most of our stars (typified by +30021), the change of 1–4-μ flux is thus mainly controlled by a change of T_e. The data shown for R Tri, however, illustrate that the radius increased sufficiently when the star changed from M5 to M7 to overcompensate for the decrease of T_e. Hence, the increase in infrared flux.

3) The amplitude of the changes at 1.04 μ may be more than, less than, or the same as those at the longer wavelengths.

In the spectral region longward of 4 μ, we do not have enough data of sufficiently good quality to be able to make definitive statements about variability. At shorter wavelengths, the behavior is what is expected for stars as cool as these, namely that the amplitude of the variations increases to wavelengths shorter than 1 μ.

VII. CONCLUSIONS

We have presented energy distributions and spectral types for a number of cool stars extending nearly as late as M10. Within this number, we have isolated a small group for which the colors are free of serious contamination by the effects of circumstellar shells and which can be used to define intrinsic energy distributions beyond M6. We have shown that there is a good relation between color temperature and spectral type and between color temperature and effective temperature. Hence, we have demonstrated the physical significance of the spectral type determined from the near-infrared VO band strength for these coolest stars.

It has been found that log $F_{2.2\mu}/\mathscr{F}$ changes very little with spectral type between M0 and M10 and allows one to obtain a good measure of the total flux simply by measuring the flux at 2.2 μ. The relation between log $F_{1.04\mu}/\mathscr{F}$ and spectral type is even flatter between M0 and M7, but changes very rapidly beyond that. Using the total fluxes and expected effective temperatures for the very coolest stars, we have shown that the angular diameters will probably be too small to be measurable by present techniques.

Many of the IRC stars in our sample, for which we have repeated observations, show evidence of variability in the 1–4-μ region, but there are no generally discernible patterns. Many also have evidence of extensive circumstellar shells, while few of the Miras do.

It is a pleasure to thank R. E. Nather, E. P. Ney, D. W. Strecker, and S. Ridgway for access to their data in advance of publication, and D. Carbon and R. F. Wing for helpful discussions.

REFERENCES

Becklin, E. E., Frogel, J. A., Hyland, A. R., Kristian, J., and Neugebauer, G. 1969, *Ap. J.* (*Letters*), **158**, L133.
Bonneau, D., and Labeyrie, A. 1973, *Ap. J.* (*Letters*), **181**, L1.
Dyck, H. M., Forbes, F. F., and Shawl, S. J. 1971, *A.J.*, **76**, 901.
Gehrz, R. D., and Woolf, N. J. 1971, *Ap. J.*, **165**, 285.
Gezari, D. Y., Labeyrie, A., and Stachnik, R. V. 1972, *Ap. J.* (*Letters*), **173**, L1.
Gillett, F. C., Merrill, K. M., and Stein, W. A. 1971, *Ap. J.*, **164**, 83.
Grasdalen, G. L., and Gaustad, J. E. 1971, *A.J.*, **76**, 231.
Hayes, D. S. 1970, *Ap. J.*, **159**, 165.
Herbig, G. H., and Zappala, R. R. 1970, *Ap. J.* (*Letters*), **162**, L15.
Hyland, A. R., Becklin, E. E., Frogel, J. A., and Neugebauer, G. 1972, *Astr. and Ap.*, **16**, 204.
Johnson, H. L. 1965*a*, *Ap. J.*, **141**, 923.
———. 1965*b*, *Comm. Lunar and Planetary Lab.*, **3**, 73.
———. 1966, *Ann. Rev. Astr. and Ap.*, **4**, 193.
Johnson, H. L., Mitchell, R. I., Iriarte, B., and Wisniewski, W. Z. 1966, *Comm. Lunar and Planetary Lab.*, **4**, 99.
Kukarkin, B. V. 1972, *Astron. Tsirk.*, No. 674.
Lockwood, G. W. 1972, *Ap. J. Suppl.*, **24**, 375.
———. 1973, in preparation.
Lockwood, G. W., and McMillan, R. S. 1971, *Proceedings of the Conference on Late-Type Stars*, ed. G. W. Lockwood and H. M. Dyck (Tucson: Kitt Peak National Observatory), Contr. No. 554, p. 171.
Lockwood, G. W., and Wing, R. F. 1971, *Ap. J.*, **169**, 63.
Lockwood, G. W., and Zinter, T. A. 1973, *A.J.*, **78**, 471.
Mendoza, V. E. E. 1967, *Bol. Obs. Tonantzintla y Tacubaya*, **4**, 114.
Nather, R. E., and Wild, P. A. T. 1973, *A.J.*, **78**, 628.
Neugebauer, G., Becklin, E., and Hyland, A. R. 1971, *Ann. Rev. Astr. and Ap.*, **9**, 67.
Neugebauer, G., and Leighton, R. B. 1969, *Two-Micron Sky Survey, A Preliminary Catalog*, NASA SP-3047.
Pease, F. G. 1931, *Ergebn. Exacten Naturwiss.*, **10**, 84.
Ridgway, S. 1973, private communication.
Smak, J. I. 1966, *Ann. Rev. Astr. and Ap.*, **4**, 19.
Strecker, D. W., Ney, E. P., and Murdock, T. L. 1973, *Ap. J.* (*Letters*), **183**, L13.
Ulrich, B. T., Neugebauer, G., McCammon, D., Leighton, R. B., Hughes, E. E., and Becklin, E. 1966, *Ap. J.*, **146**, 288.
Vogt, S. S. 1973, *A.J.*, **78**, 389.
Wilson, W. J., and Barrett, A. H. 1971, *Proceedings of the Conference on Late-Type Stars*, ed. G. W. Lockwood and H. M. Dyck (Tucson: Kitt Peak National Observatory), Contr. No. 554, p. 77.
Wing, R. F. 1967, unpublished Ph.D. dissertation, University of California at Berkeley.
Wing, R. F., and Lockwood, G. W. 1973, *Ap. J.*, **184**, 873.
Zellner, B. H., and Serkowski, K. 1972, *Pub. A.S.P.*, **84**, 619.